

Effects of a contoured articular prosthetic device on tibiofemoral peak contact pressure: a biomechanical study

Christoph Becher · Roland Huber ·
Hajo Thermann · Hans H. Paessler ·
Gobert Skrbensky

Received: 12 June 2007 / Accepted: 30 August 2007 / Published online: 13 October 2007
© Springer-Verlag 2007

Abstract Many middle-aged patients are affected by localized cartilage defects that are neither appropriate for primary, nor repeat biological repair methods, nor for conventional arthroplasty. This in vitro study aims to determine the peak contact pressure in the tibiofemoral joint with a partial femoral resurfacing device (HemiCAP[®], Arthrosurface Inc., Franklin, MA, USA). Peak contact pressure was determined in eight fresh-frozen cadaveric specimens using a Tekscan sensor placed in the medial compartment above the menisci. A closed loop robotic knee simulator was used to test each knee in static stance positions (5°/15°/30°/45°) with body weight ground reaction force (GRF), 30° flexion with twice the body weight (2tBW) GRF and dynamic knee-bending cycles with body weight GRF. The ground reaction force was adjusted to the living body weight of the cadaver donor and maintained throughout all cycles. Each specimen was tested under four different conditions: Untreated, flush HemiCAP[®] implantation, 1-mm proud implantation and 20-mm defect. A paired sampled *t* test to compare means

(significance, $P \leq 0.05$) was used for statistical analysis. On average, no statistically significant differences were found in any testing condition comparing the normal knee with flush device implantation. With the 1-mm proud implant, statistically significant increase of peak contact pressures of 217% (5° stance), 99% (dynamic knee bending) and 90% (30° stance with 2tBW) compared to the untreated condition was seen. No significant increase of peak contact pressure was evaluated with the 20-mm defect. The data suggests that resurfacing with the HemiCAP[®] does not lead to increased peak contact pressure with flush implantation. However, elevated implantation results in increased peak contact pressure and might be biomechanically disadvantageous in an in vivo application.

Keywords Osteochondral defect · Tibiofemoral joint · Articular prosthetic device · Peak contact pressure · Knee biomechanics

Introduction

In 50% of the patients undergoing routine arthroscopy, articular cartilage defects are detected [6]. The majority of cartilage lesions are observed in patients over the age of 40 years [6, 11]. Approximately 20% of these lesions were categorized as full thickness cartilage defects (Grade IV) [6]. The average defect size in 1,000 knee arthroscopies was 2.1 cm² with 42% of these defects being between 2 to 4 cm² in area [11]. Location of the lesions are predominantly on the medial femoral condyle [6, 11]. Clinical and experimental studies have shown that a relationship exists between larger defect size and degeneration of the articular surface. Linden et al. [19] demonstrated that the presence of a significant chondral defect is associated with a much

C. Becher (✉)
Department of Orthopaedic Surgery,
Phillips University Marburg, Baldinger Str,
35043 Marburg, Germany
e-mail: becher.chris@web.de

R. Huber · G. Skrbensky
Bone and Joint Biomechanic Laboratory,
Medical University of Vienna, Waehringergürtel 18-20,
1090 Wien, Austria

H. Thermann · H. H. Paessler
Centre for Knee and Foot Surgery/Sports Trauma,
ATOS Clinic Center, Bismarckstr. 9-15,
69115 Heidelberg, Germany

higher incidence of osteoarthritis than occurs in the general population. Hughston et al. [13] showed that larger osteochondral defects are associated with a poorer clinical outcome than smaller defects.

The treatment for articular cartilage defects offers a great variety of options depending on the severity of the damage. The main factors to be considered are the patient age, the size of the lesion, the location of the defect, and further damage to the joint. Biological repair techniques, such as autologous chondrocyte transplantation, osteochondral transplantation (OATS, Mosaicplasty) and marrow stimulation techniques are proposed for the treatment of localized cartilage defects in younger patients with a normal weight bearing axis and no further damage to the joint [3, 8]. However, many middle aged patients are affected by localized cartilage damage and are neither fit for biological repair methods, nor for traditional resurfacing techniques such as unicompartmental or total joint replacement. A contoured articular prosthetic unicompylar femoral resurfacing prosthesis (HemiCAP[®], ArthroSurface Inc., Franklin, MA, USA) was developed to offer a treatment option among the currently used modalities. It is intended for use as a partial resurfacing device of the femoral condylar surface of the knee when only one compartment is affected by posttraumatic, degenerative disease or necrosis associated with large unstable articular defects with significant subchondral bone exposure.

However, it is unknown if the femoral resurfacing device leads to increased peak contact pressure to the opposing biological structures such as meniscus and articular cartilage of the tibial plateau.

The purpose of our study was to determine peak contact pressures in the medial compartment of human cadaveric knees under different loading conditions comparing the normal articular surface to flush and proud HemiCAP[®] implantation and defect. Based on the experimental study, biomechanical device safety on opposing structures can be assessed and a guideline might be given to the clinician for prosthetic implantation while avoiding potentially damaging effects.

Materials and methods

Knee joints

A total of eight fresh-frozen knee cadaver specimens (3 pairs, 2 single) were used for data collection in this study. The specimens were obtained from donors, who consented in writing during their lifetime to the use of their body for research and education. The average age of the seven male and one female specimen was 71 years (range 61–81) with an average weight of 71 kg (range 62–85).

Specimens were selected after inspection of the medial compartment according to the following criteria: Intact femorotibial cartilage, intact meniscus, and intact collateral and cruciate ligaments. Thirteen specimens were excluded following these criteria. Another six specimens were excluded due to specimen failure during the testing procedure: The reason for exclusion was fracture of the femur or tibial plateau (2 specimens), rupture of the anterior cruciate ligament (2 specimens) or rupture of the patella tendon (2 specimens). All specimen failures were female human cadaver knees.

Technology

A specially designed knee simulator was used for this study (Fig. 1). Similar to *in vivo* conditions, the main system composed of artificial muscle, force transducer sensor, the joint angle detection and the ground reacting force form a closed loop. The ground reaction force is adjustable according to the donor's weight. The knee simulator consists of a loading frame (MTS 858 Bionix, MTS Systems,

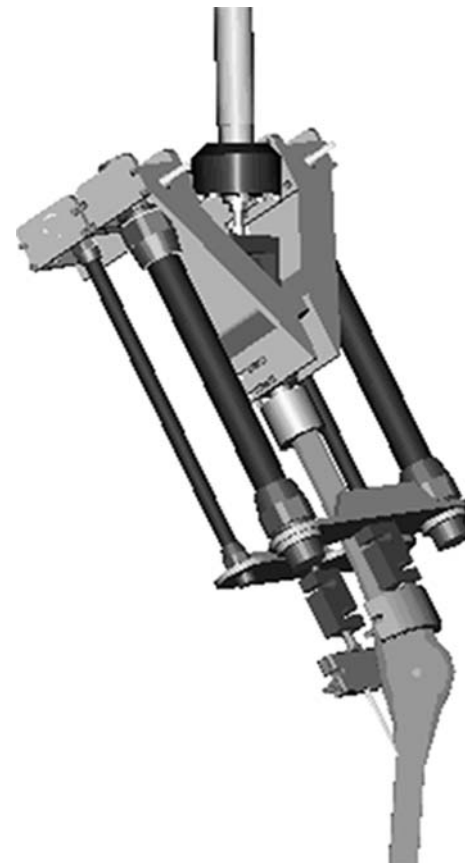


Fig. 1 Schematic drawing of the knee simulator that was used for this study

Eden Prairie, MN, USA) with a long stroke main actuator driven by a hydraulic pump unit (MTS 505.11 silent flow) to simulate body weight and the vertical hip displacement in the mechanical axis of the lower limb. Ankle joint simulation is performed with a hinge joint with one free motion axis. The possible rotation during the movement occurs in the artificial hip joint as if standing with fixed shoe contact. A load transducer is fixed between the mounting plate and ankle joint to detect the vertical ground reacting force (U3 load cell, Hottinger-Baldwin, Darmstadt, Germany). Two smaller actuators apply loads, which simulate the quadriceps force. The tendons of the quadriceps muscle are attached to customized curved cryo-clamps, which avoid patella tilting. These cryo-clamps are connected to a waterproof force transducer (SSM-AJ 500, Interface, Scottsdale, AZ, USA) and connected to an artificial muscle (Fluidic muscle MAS, Festo, Esslingen, Germany). The mathematical model shows that the properties of this fluidic muscle is comparable with a skeletal muscle [28].

A 0.1 mm thin electronic pressure measuring sensor (K-scan 4000, Tekscan, Boston, MA, USA) was placed in the medial compartment above the menisci and fixed with sutures in a manner that no displacement was possible. The sensor consists of load-sensing regions oriented in a grid with 1.27 mm spacing between rows and columns. Each region is referred to a sensel with piezo-resistive pigments to determine the total compressive load within that region. The size of the sensor is 28×33 mm with 62 sensels/cm². The K-scan sensor was successfully used in comparable applications by several authors [18, 21, 25, 31].

The HemiCAP[®] implant (Arthrosurface Inc., Franklin, MA, USA) is a contoured articular prosthetic (CAP) unicondylar femoral resurfacing prosthesis consisting of two components, a fixation component and an articular component, that mate together via a taper interlock to provide stable and immobile fixation of the implant and stress-bearing contact at the bone/prosthetic interface. The fixation component is a modified titanium cancellous screw with a tapering distal tip, a full-length cannulation, and a proximal female taper bore. The articular component is a

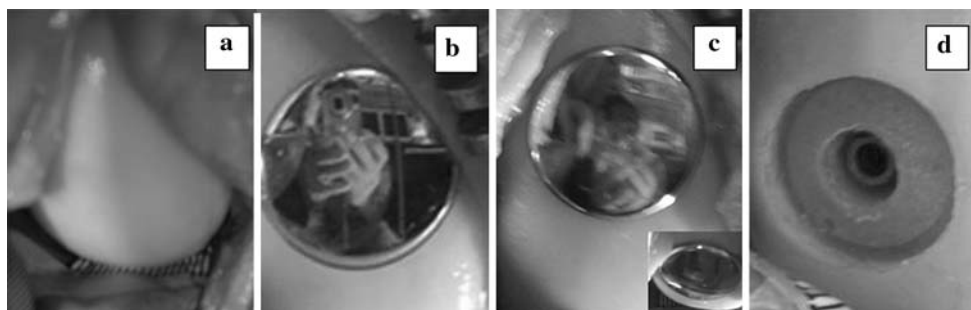
dome-shaped component manufactured of a Cobalt–Chromium–Molybdenum alloy with titanium plasma spray coverage on the underside for bony in-growth. Each diameter comes in a variety of incremental offset sizes which correspond to the superior/inferior and medial/lateral radius of curvatures at the implant site. The size of the implant used in this study was 20 mm in diameter with different offset sizes, matching the individual specimen joint curvature.

Testing protocol

The specimens were aligned using a fixed laser beam to achieve correct alignment in the mechanical axis of the lower limb. The mechanical axis was defined by a line through the center of the head of the artificial hip joint, the center of the knee joint and the center of the hinge joint representing the artificial ankle. For calibration of the sensor the ankle hinge joint was secured with two aluminum plates perpendicular to the ground. Thereby the knee was fixed in full extension. Each sensor was individually preconditioned and calibrated intra-articular with a two-point calibration method at 700 and 1,500 N according to manufacturer's guidelines. Definitions of the correct angles of the actual knee position were adjusted with a custom-made goniometer and by the displacement-controlled main rod. During the test cycles the cadaver were sprayed with saline solution to prevent dehydration.

The specimens were tested in four different conditions: (1) Untreated knee, (2) Flush HemiCAP[®] (20 mm) implanted in the central weight bearing area of the medial femoral condyle, (3) 1 mm proud implantation to adjacent cartilage, (4) 20 mm defect (Fig. 2a–d). Each knee was tested in static knee stance positions (5°, 15°, 30°, 45°) with body weight ground reaction force, 30° flexion with two times body weight ground reaction force and during a knee-bending dynamic cycle (10 cycles) with body weight ground reaction force. The setting of ground reaction force to be achieved during the trial was adjusted to the living body weight of the donator of the cadaver (e.g.

Fig. 2 Different testing conditions (a Untreated; b Flush; c 1 mm; d Defect)

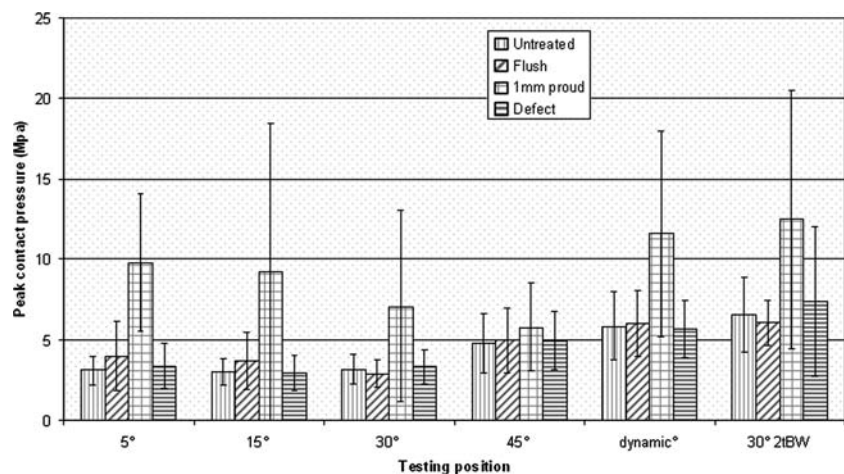


70 kg ~ 700 N). The loading rate for exploring the dynamic contact pressures was 0.1 Hz/s.

Operative technique

All specimens were released at their femoral fixation during preparation of a new testing condition. The exact position was marked and recorded to maintain specimen position in the knee simulator across all testing conditions. The position of the sensor did not change during the preparation. All procedures were performed by the same investigator (CB). The medial femoral condyle was exposed by a medial parapatellar incision. The knee was flexed to 90° to expose the central weight-bearing portion. A drill guide was used to place a pin perpendicular to the joint surface representing the center of the defect. The center of the defect was determined by measuring the condylar width and bisecting the distance. The cannulated instrumentation set ensured that the vertical axis was maintained throughout the procedure. After drilling a pilot hole, the fixation component was inserted. A contact probe determined the radius of curvature in two planes. With a matching reamer, the site for the implantation was prepared and a sizing trial with corresponding offsets inserted. The selected device was oriented in the correct planes and connected to the anchoring screw with a tapered lock. In order to allow for careful removal of the articular component, the guide wire was initially drilled through the condyle and remained inside the cannulated screw during the trial. After testing with flush implantation (Fig. 2b), the device was removed with the guide wire. The anchoring screw was elevated with a counter-clockwise quarter turn representing 1 mm and the device re-inserted for positioning 1 mm above the adjacent cartilage (Fig. 2c). Defect condition was tested after removing the guide wire and device leaving a 20-mm osteochondral defect of 3–4 mm depth (Fig. 2d).

Fig. 3 Mean peak contact pressures with one standard deviation



Data analysis

Data were obtained using I-Scan software 4.23 (Tekscan, Boston, MA, USA). Peak contact pressure was assessed and recorded as the highest value at each stance position and during the dynamic knee-bending cycle. Mean, median and standard deviation values were evaluated using MS-Excel 2003 (Microsoft Inc., Redmond, WA, USA) and SPSS 11.0 (SPSS Inc., Chicago, IL, USA). For statistical analysis a paired sampled *t* test to compare means (significance, $P \leq 0.05$) was used.

Results

Continuous data were obtained at every trial. No difference in the quality of data collection was seen comparing the stance positions or dynamic testing.

The highest mean peak contact pressures were noted with the implant being 1 mm proud (Fig. 3; Table 1). Statistically significant increase of peak contact pressures of 217% (5° stance; $P \leq 0.004$), 99% (dynamic knee bending; $P \leq 0.02$) and 90% (30° stance with 2tBW; $P \leq 0.03$) compared to the untreated condition was seen. Average results of 45° static testing demonstrated only slightly higher values compared to the other testing positions, indicating that the implant was non-weight bearing and lost contact to the sensor at this position (Fig. 3; Table 1).

On average, comparison of the untreated normal knee with flush device implantation demonstrated neither statistically significant differences in peak contact pressure during the dynamic knee-bending cycle nor static testing (5°, 15°, 30°, 45°) or two times body weight GRF at 30° static testing (Table 1). Six out of eight specimens demonstrated similar peak contact pressures in both testing conditions, two specimens showed a noticeable increase in

Table 1 Peak contact pressures at different testing conditions

Testing position	Testing condition	Peak contact pressure (Mpa)	Mean difference to untreated (%)	P value
5°	Untreated	3.09 ± 0.86 (3.05, 1.92–4.86)	N/A	N/A
	Flush	3.98 ± 2.19 (3.59, 2.15–9.02)	29	NS
	1 mm proud	9.80 ± 4.37 (9.36, 4.70–18.37)	217	≤0.004
	Defect	3.35 ± 1.39 (3.39, 1.90–5.83)	8	NS
15°	Untreated	3.01 ± 0.81 (2.95, 2.01–4.11)	N/A	N/A
	Flush	3.69 ± 1.79 (3.89, 1.38–7.06)	23	NS
	1 mm proud	9.19 ± 9.27 (5.87, 2.10–30.49)	205	NS
	Defect	2.94 ± 1.07 (2.84, 1.69–5.09)	–2	NS
30°	Untreated	3.18 ± 0.94 (3.52, 1.46–4.26)	N/A	N/A
	Flush	2.89 ± 0.85 (3.02, 1.03–3.83)	–9	NS
	1 mm proud	7.07 ± 5.97 (5.24, 1.03–19.81)	122	NS
	Defect	3.31 ± 1.06 (3.11, 2.05–5.34)	4	NS
45°	Untreated	4.77 ± 1.85 (4.23, 2.66–7.90)	N/A	N/A
	Flush	4.96 ± 2.02 (4.18, 2.79–7.92)	4	NS
	1 mm proud	5.79 ± 2.76 (5.54, 2.01–11.82)	21	NS
	Defect	4.94 ± 1.81 (4.65, 2.05–7.54)	4	NS
Dynamic	Untreated	5.84 ± 2.12 (5.14, 3.85–9.82)	N/A	N/A
	Flush	6.02 ± 2.05 (5.21, 3.46–8.97)	3	NS
	1 mm proud	11.61 ± 6.39 (10.50, 6.22–25.46)	99	≤0.02
	Defect	5.68 ± 1.76 (5.11, 3.76–8.24)	–3	NS
30° 2tBW	Untreated	6.57 ± 2.31 (6.01, 4.09–11.15)	N/A	N/A
	Flush	6.05 ± 1.40 (5.82, 4.68–8.97)	–8	NS
	1 mm proud	12.49 ± 8.02 (9.67, 5.83–30.49)	90	≤0.03
	Defect	7.38 ± 4.68 (5.31, 4.75–17.70)	12	NS

Values given as mean ± SD (median, range)

NS not significant

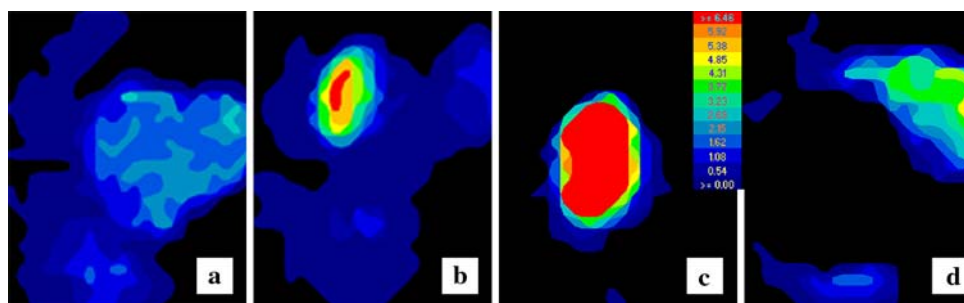


Fig. 4 Peak contact pressure at 15° static knee stance position with single body weight of specimen No. 2. The color represents the spectrum of pressures (high pressure-red; low pressure-blue). From left to right the different testing conditions are displayed (a Untreated,

b Flush, c 1 mm proud, d Defect). Marked increase of peak contact pressure at the edge of the implant to the adjacent cartilage is demonstrated (b)

peak contact pressures (flush device implantation) averaging 29% during 5° static testing and 23% in 15° static testing. Data evaluation of the two respective trials with outlying measurements demonstrated edge loading at the border of the implant to the adjacent cartilage (Figs. 4b, 5b).

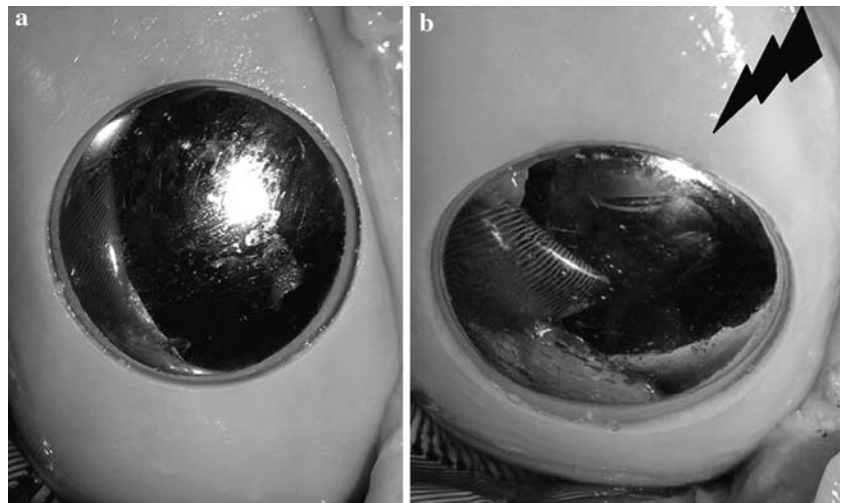
No significant increase of peak contact pressures was evaluated with the 20-mm osteochondral defect. However, average increase by 8% (5° stance) and 12% (30° stance with 2tBW) were found compared to untreated-condition (Table 1). Furthermore, maximum values were higher

compared to untreated condition (except 45° stance position and dynamic testing cycle).

Discussion

The patient aged over 40 years with a full thickness chondral or osteochondral defect reflects a serious problem for the orthopedic surgeon. Considered as being too old for biological repair of the defect, primarily the

Fig. 5 Picture of specimen No. 2 before testing with flush implantation of the device in front view (a) and top view (b). The arrow indicates the area of peak contact pressure displayed in Fig. 4b



patients are mostly managed with conservative, non-surgical treatment including weight reduction, physical therapy to increase and support musculature, unloading braces and medications such as NSAID's, intraarticular injections (Corticosteroids, Hyaluronic acid, etc.) and dietary supplements.

However, conservative treatment at best ameliorates the symptoms. Biomechanical studies have shown that untreated osteochondral defects may result in increased contact pressures [4, 7, 17]. Animal models proved that untreated osteochondral defects undergo progressive degenerative changes [5, 14]. Whereas smaller defects might have the capacity for healing [5], it was shown that larger defects resulted in resorption of the osseous walls of the defect, the formation of a large cavitory lesion, and the collapse of the surrounding articular cartilage and subchondral bone as well as to degeneration of the opposing tibial articular surface [5, 14]. A “threshold” effect for localized full thickness defects was described with rim concentration around the lesion becoming a factor for defects greater than 10 mm in diameter (0.79 cm^2) [7].

Defect repair is therefore regarded crucial to prevent or delay progressive degenerative joint destruction. However, unicompartmental or total knee arthroplasty represent procedures of final resort for some of the affected patients. The HemiCAP[®] resurfacing prosthesis (Arthrosurface Inc., Franklin, MA, USA) offers an interim or alternative treatment strategy for the middle-aged patient with a full thickness cartilage defect. However, effects of a metallic implant articulating with intact opposing tibial articular cartilage and meniscus remain largely unanswered to date. An experimental study assessing the functional and biological response to its use in a goat model resulted in good clinical outcomes. One year after implantation, gross necropsy and histologic data implied the biocompatibility and functionality of the implant. No ongoing degenerative joint

disease was apparent [15]. Macroscopic and histological analysis showed that the cartilage around the implant was largely intact although some focal fraying and erosion and limited meniscal damage was observed. The opposing tibial plateau cartilage surface was generally intact but exhibited some focal erosions of variable depth [15]. The outcome was substantially better by comparison to other reported experimental animal studies in goats with untreated full-thickness defects [14, 29]. A patellar resurfacing prosthesis resulted at an average of 8.1 years in 71% good or excellent cases with no progressive degenerative changes in the non-resurfaced apposing femoral articular cartilage as long as 16 years [9]. A successful clinical outcome with a metallic distal femoral prosthesis articulating directly against the menisci and proximal tibial plateau over 30 years was documented in a case report [12].

Our results revealed significant increase of peak contact pressures with the implant being proud to the surrounding cartilage compared to the untreated condition with an average maximum increase of 217% and 205% at 5° and 15° stance compared to untreated knees. Results in a biomechanical model using osteochondral plugs for the treatment of osteochondral defects demonstrated increased contact pressures up to 57% compared to intact condition in elevated or angled plugs with an edge placed higher than the adjacent cartilage [16, 17]. Thus, increased peak contact pressures may suggest biomechanical disadvantages and may cause damage to opposing structures. Several in vitro studies have shown increased chondrocyte apoptosis and matrix deformation after peak stress loading of bovine and human articular cartilage [2, 20, 22, 23]. However, quantitative thresholds above which elevated pressure is detrimental are not defined yet.

Flush implantation showed no statistical increase of peak contact pressures compared to untreated. However, in two specimens we found marked increase of peak contact

pressures at the edge of the implant. Evaluation of the pictures of the specimen after the trial showed that the implant did not appear to be proud to the adjacent cartilage in the front view (Fig. 5a). However, in the top view it seemed that the implant was in level with the adjacent cartilage or even slightly elevated at the point of increased peak contact pressure (Fig. 5b). Reduced quality of the adjacent cartilage directly next to the measured peak contact pressure might have lead to less resistive cartilage capacity allowing for edge loading. Thus, it appears to be crucial to have healthy surrounding cartilage around the implant and to spend special care during the implantation process so that the implant is not elevated above the adjacent cartilage at any point. Koh et al. [16] showed in their biomechanical study, that slightly recessed osteochondral grafts with the highest edge placed flush to neighboring cartilage demonstrated nearly normal contact pressures, whereas elevated angled grafts produced increased contact pressures. Our results confirm the observation concluding that slightly recessed implantation should be considered if flush implantation cannot be accomplished.

Defect situation in our study did not result in significant increase of peak contact pressures. Rim stress concentration has been described by several authors in their biomechanical models evaluating the contact pressures in full thickness cartilage defects [4, 5, 7, 16, 17, 26]. However, results were uncertain whether the peak contact pressure increases at the rim of the defect. Whereas Koh et al. [17] reported average increase of peak contact pressure by 23% compared to the untreated condition, Raimondi et al. [26] and Nelson et al. [24] found no elevated contact stresses at the rim of the defect. These different observations might be caused by the different deformation of defect rims under a given load, especially in larger defects than in smaller defects. The relationship of defect size to the condylar surface may be also a factor [7]. The methodology concerning the model (animal or human being cadaver), the experimental setup (loading mechanics, dynamic or static, etc.) and the pressure-sensitive sensor and performance of the trial have also to be considered.

Limitations of this study have to be considered and include the following. (1) This is a human cadaver study and biomechanical model. Only approximation of the living system can be achieved. However, the pre-selection of the applied load by the ground reaction force gave the opportunity to load the specimens with the known body weight of the donor, and thus better approximate the forces that occur in the living system [30]. Furthermore, the knee bending dynamic measurement may have provided a more accurate reproduction of physiologic weight-bearing activity. However, the complexity of weight-bearing motions

including all the muscle groups for knee motion could not be reproduced. Applied forces were too high for female human cadaver knees resulting in a high specimen's failure rate. (2) Peak contact pressures were determined by an electronic pressure sensitive sensor. The reliability of the K-scan sensor was verified in several studies [10, 18, 21, 31]. In comparison to other measuring devices (Fuji Photo Film), the Tekscan K-sensor proved to be superior [10, 27]. Limitations of the sensor include the thickness (0.1 mm), its sensitivity to temperature changes, its disposition for crinkling and the establishment of the position [1]. Although the position of the sensor was accurately secured, a small amount of displacement and crinkling could not be excluded. A certain amount of loss of sensitivity during the different testing conditions and imprecise calibration due to the different surface materials (metal on cartilage, cartilage on cartilage) have to be considered. Some drop of data point was observed at some specimen. However, peak contact values seemed not to be affected. (3) Stable, reproducible ground reaction force in full extension could not be established by the simulator. The quadriceps tendon could not be adequately tensioned in this position. (4) Implantation of the device was performed in the central weight-bearing area. Results might be different for the implantation in different areas of the medial femoral condyle or lateral condyle.

In conclusion, the data suggest that resurfacing with the HemiCAP[®] with flush implantation does not lead to significantly increased peak contact pressure. However, elevated implantation results in significantly increased peak contact pressure and might be biomechanically disadvantageous in an in vivo application. Further research is necessary to evaluate the effects of the prosthetic device on contact pressures after loss of meniscus function and in longer continuous dynamic testing.

References

1. Beck PR, Thomas AL, Farr J, Lewis PB, Cole BJ (2005) Trochlear contact pressures after anteromedialization of the tibial tubercle. *Am J Sports Med* 33:1710–1715
2. Brand RA (2005) Joint contact stress: a reasonable surrogate for biological processes? *Iowa Orthop J* 25:82–94
3. Brittberg M, Lindahl A, Nilsson A, Ohlsson C, Isaksson O, Peterson L (1994) Treatment of deep cartilage defects in the knee with autologous chondrocyte transplantation. *N Engl J Med* 331:889–895
4. Brown TD, Pope DF, Hale JE, Buckwalter JA, Brand RA (1991) Effects of osteochondral defect size on cartilage contact stress. *J Orthop Res* 9:559–567
5. Convery FR, Akeson WH, Keown GH (1972) The repair of large osteochondral defects. An experimental study in horses. *Clin Orthop Relat Res* 82:253–262
6. Curl WW, Krome J, Gordon ES, Rushing J, Smith BP, Poehling GG (1997) Cartilage injuries: a review of 31,516 knee arthroscopies. *Arthroscopy* 13:456–460

7. Guettler JH, Demetropoulos CK, Yang KH, Jurist KA (2004) Osteochondral defects in the human knee: influence of defect size on cartilage rim stress and load redistribution to surrounding cartilage. *Am J Sports Med* 32:1451–1458
8. Hangody L, Fules P (2003) Autologous osteochondral mosaicplasty for the treatment of full-thickness defects of weight-bearing joints: ten years of experimental and clinical experience. *J Bone Joint Surg Am* 85-A(Suppl 2):25–32
9. Harrington KD (1992) Long-term results for the McKeever patellar resurfacing prosthesis used as a salvage procedure for severe chondromalacia patellae. *Clin Orthop Relat Res* 201–213
10. Harris ML, Morberg P, Bruce WJ, Walsh WR (1999) An improved method for measuring tibiofemoral contact areas in total knee arthroplasty: a comparison of K-scan sensor and Fuji film. *J Biomech* 32:951–958
11. Hjelle K, Solheim E, Strand T, Muri R, Brittberg M (2002) Articular cartilage defects in 1,000 knee arthroscopies. *Arthroscopy* 18:730–734
12. Hodge WA (1991) Vitallium-mold arthroplasty of the knee. A case report with 30-year follow-up study. *J Arthroplasty* 6:195–197
13. Hughston JC, Hergenroeder PT, Courtenay BG (1984) Osteochondritis dissecans of the femoral condyles. *J Bone Joint Surg Am* 66:1340–1348
14. Jackson DW, Lalor PA, Aberman HM, Simon TM (2001) Spontaneous repair of full-thickness defects of articular cartilage in a goat model. A preliminary study. *J Bone Joint Surg Am* 83-A:53–64
15. Kirker-Head CA, Van Sickle DC, Ek SW, McCool JC (2006) Safety of, and biological and functional response to, a novel metallic implant for the management of focal full-thickness cartilage defects: preliminary assessment in an animal model out to 1 year. *J Orthop Res* 24:1095–1108
16. Koh JL, Kowalski A, Lautenschlager E (2006) The effect of angled osteochondral grafting on contact pressure: a biomechanical study. *Am J Sports Med* 34:116–119
17. Koh JL, Wirsing K, Lautenschlager E, Zhang LO (2004) The effect of graft height mismatch on contact pressure following osteochondral grafting: a biomechanical study. *Am J Sports Med* 32:317–320
18. Lee SJ, Aadalen KJ, Malaviya P, Lorenz EP, Hayden JK, Farr J, Kang RW, Cole BJ (2006) Tibiofemoral contact mechanics after serial medial meniscectomies in the human cadaveric knee. *Am J Sports Med* 34:1334–1344
19. Linden B (1977) Osteochondritis dissecans of the femoral condyles: a long-term follow-up study. *J Bone Joint Surg Am* 59:769–776
20. Loening AM, James IE, Levenston ME, Badger AM, Frank EH, Kurz B, Nuttall ME, Hung HH, Blake SM, Grodzinsky AJ, Lark MW (2000) Injurious mechanical compression of bovine articular cartilage induces chondrocyte apoptosis. *Arch Biochem Biophys* 381:205–212
21. Matsuda S, White SE, Williams VG, 2nd McCarthy DS, Whiteside LA (1998) Contact stress analysis in meniscal bearing total knee arthroplasty. *J Arthroplasty* 13:699–706
22. Milentijevic D, Torzilli PA (2005) Influence of stress rate on water loss, matrix deformation and chondrocyte viability in impacted articular cartilage. *J Biomech* 38:493–502
23. Morel V, Berutto C, Quinn TM (2006) Effects of damage in the articular surface on the cartilage response to injurious compression in vitro. *J Biomech* 39:924–930
24. Nelson BH, Anderson DD, Brand RA, Brown TD (1988) Effect of osteochondral defects on articular cartilage. Contact pressures studied in dog knees. *Acta Orthop Scand* 59:574–579
25. Ostermeier S, Holst M, Hurschler C, Windhagen H, Stukenborg-Colsman C (2007) Dynamic measurement of patellofemoral kinematics and contact pressure after lateral retinacular release: an in vitro study. *Knee Surg Sports Traumatol Arthrosc* 15:547–554
26. Raimondi MT, Pietrabissa R (2005) Contact pressures at grafted cartilage lesions in the knee. *Knee Surg Sports Traumatol Arthrosc* 13:444–450
27. Szivek JA, Cutignola L, Volz RG (1995) Tibiofemoral contact stress and stress distribution evaluation of total knee arthroplasties. *J Arthroplasty* 10:480–491
28. Tondu B, Lopez P (2000) Modeling and control of McKibben artificial muscle robot actuators. *IEEE Control Syst* 20:15–38
29. van Susante JL, Buma P, Schuman L, Homminga GN, van den Berg WB, Veth RP (1999) Resurfacing potential of heterologous chondrocytes suspended in fibrin glue in large full-thickness defects of femoral articular cartilage: an experimental study in the goat. *Biomaterials* 20:1167–1175
30. von Skrbensky G, Huber R (2006) Vienna 2.2 Knee Joint Simulator for long-term in vitro testing. *J Biomech* 39:S50
31. Wirz D, Becker R, Li SF, Friederich NF, Muller W (2002) Validation of the Tekscan system for static and dynamic pressure measurements of the human femorotibial joint. *Biomed Tech (Berl)* 47:195–201